EOLI
Efficient Operation of Urban Wastewater Treatment Plants

Deliverable D1.3
Report on the model selection, parameter identification and validation

WP1. Process experiments
Responsible: Germán Buitrón (UNAM)
Involved partners UNAM, POLIMI, UU

By
Manuel J. Betancur, Jaime A. Moreno, Iván Moreno-Andrade and Germán Buitrón (UNAM)
Nicola Fiocchi, Elena Ficara and Roberto Canziani (POLIMI)
Adrián Ferrari and Soledad Gutiérrez(UU)

Contract Number ICA4-CT-2002-10012

TABLE OF CONTENTS

CASE I UNAM. TOXIC WASTEWATER **3**

INTRODUCTION **3**

EXPERIMENT SELECTION **3**

MODEL STRUCTURE **3**

IDENTIFICATION PROCEDURES **5**

RESULTS AND VALIDATION **6**

BIOMASSES COMPARISON **11**

CONCLUSIONS **13**

ANNEX 1. EXPERIMENTAL FILES NAMES AND CLASSIFICATION 14
ANNEX 2. PRECISION OF MEASUREMENTS 17
ANNEX 3. ESTIMATION OF YIELD COEFFICIENTS 18
ANNEX 4. DEFINITIONS AND UNITS 19
ANNEX 5. KINETIC PARAMETERIZATION 20
ANNEX 6. MODELING ASSUMPTIONS 22
ANNEX 7. INITIAL CONDITIONS AND ESTIMABLE PARAMETERS 24
ANNEX 8. D.O. SENSOR MODEL 26
ANNEX 9. SOFTWARE, FITTING CRITERIA AND STATISTICAL GUIDELINES 27
ANNEX 10. RELATED DOCUMENTS (REPORTS, GRAPHS, DATA, CODE…) 30

CASE II POLIMI. NUTRIENTS REMOVAL **31**

EXPERIMENTS FOR MODEL CALIBRATION AND VALIDATION *31*
ANALYTICAL METHODS 31
EXPERIMENTS PERFORMED DURING THE FIRST YEAR 33
Experiment 1 : Standard conditions *33*
Experiment 2 : Standard conditions replicate *34*
Experiment 3 : COD/N – 50% *35*
Experiment 4 : COD/N – 35% *35*
Experiment 5 : COD/N + 35% *36*
Experiment 6: COD/N -20% *36*
Experiment 7: COD/N +20% *37*
Experiment 8: COD,N +25% *38*
Experiment 9: COD, N +50% *38*
Experiment 10: COD/N +50% *40*
Experiment 11 COD, N +75% *41*
Experiment 12: COD, N +75% *41*
Experiment 13: COD, N +50% *42*
Experiment 15: Acute toxicant *43*
Experiment 16: air flow rate +50% *44*
Experiment 17 (29/01/04) air flow rate -50% *44*
Experiment 18 - standard conditions *45*
Experiment 19: acute toxicant *45*
Experiment 20 acute toxicant *46*
Experiment 21 new loading conditions *46*
BATCH EXPERIMENTS FOR THE STUDY OF THE BIOSORPTION PHENOMENON 47
Material and Methods *47*
RESULTS 48
Synthetic wastewater as the organic carbon source *48*
Solution of milk serum as the organic carbon source *50*
CONCLUSIONS 52

REFERENCES **53**

CASE I UNAM. TOXIC WASTEWATER

INTRODUCTION

This work reports the identification of EOLI Model one (EM1) using a new set of experiments (ID3, ID4, VAL2) and a new procedure (C3). This C3 proposal adds two refinements to the model. It includes the sensor filtering effect on the oxygen signal and includes also a modification to the Specific Biomass Growth Rate curve for very low substrate concentrations. A procedure D3 without these additions is also performed to those same experiments for comparison purposes. The user then may now choose, for example, between the simpler D3 type or, if more stringent fitting needs arise, the C3 type instead.

To test the hypothesis that different biomasses may have significantly different kinetic models, a mixture of all ID experiments available was made, and a unified EM1-BC3 was generated. It is a mixture of procedures B and C and is the best single representation for all experiments in set (ID1, ID2, ID3, ID4, VAL1 and VAL2).

In total 3 new EM1 candidates BC3, C3 and D3 are now added to the repertory of models. For completeness, all annexes and data tables from former reports are also included and, when appropriated, updated with the new procedures results.

EXPERIMENT SELECTION

After careful examination UNAM's WP1 team recommended a validation VAL2 experiment for set (ID3, ID4). These experiments belong to the "Starvation" mode. However all comply with standard specifications. The biomass used in all of them is the same, but different to that used in (ID1, ID2, VAL1) for former procedures A and B.

Annex 1 shows the full names and classification of all experiments.

MODEL STRUCTURE

Equation 1 represents the basic structure of the SBR mathematical model, for both the fill-reaction and full-reaction phases in all model candidates. Equation 2 complements it by representing the effect of D.O. Sensor on oxygen signal for candidate "C". Such effect is approximated as a second order filter. Definitions and units are found in Annex 4.

$$\dot{X} = \mu X - k_d X \frac{q_{in}}{V}$$

$$\dot{S}_C = -k_1 \mu X + (S_{C,in} - S_C)\frac{q_{in}}{V} \qquad \text{Eq.(1)}$$

$$\dot{S}_O = -k_2 \mu X - bX + K_L a^* (S_{Os} - S_O) + (S_{O,in} - S_O)\frac{q_{in}}{V}$$

$$\dot{V} = q_{in}$$

$$\dot{S}_{Oa} = (S_O - S_{Oa})/\tau_a \qquad \text{Eq.(2)}$$

$$\dot{S}_{Osen} = (S_{Osen} - S_{Oa})/\tau_b$$

Equation 3 represents the *Haldane* graph for the Specific Biomass Growth Rate as function of *Substrate* and *Dissolved Oxygen*. Equation 4 represents the Oxygen limitation dependence and Equation 5 represents the proposed modification for the inhibitory substrate dependence (Betancur et al, 2002; Moreno et al 2003). Figure 1 shows a graph for Equation 5 displaying the threshold piece-wise discontinuity proposed.

$$\square = \square_S \square_{DO} \qquad \text{Eq.(3)}$$

$$\square_{DO} = \frac{O}{O + K_o} \qquad \text{Eq.(4)}$$

$$\square = \begin{cases} \dfrac{\square_0 S_C}{K_S + S_C + S_C^{\,2} / K_I} & for \quad S_C \geq S_t \\ \square_t S_C / S_t & for \quad S_C \prec S_t \end{cases} \qquad \text{Eq.(5)}$$

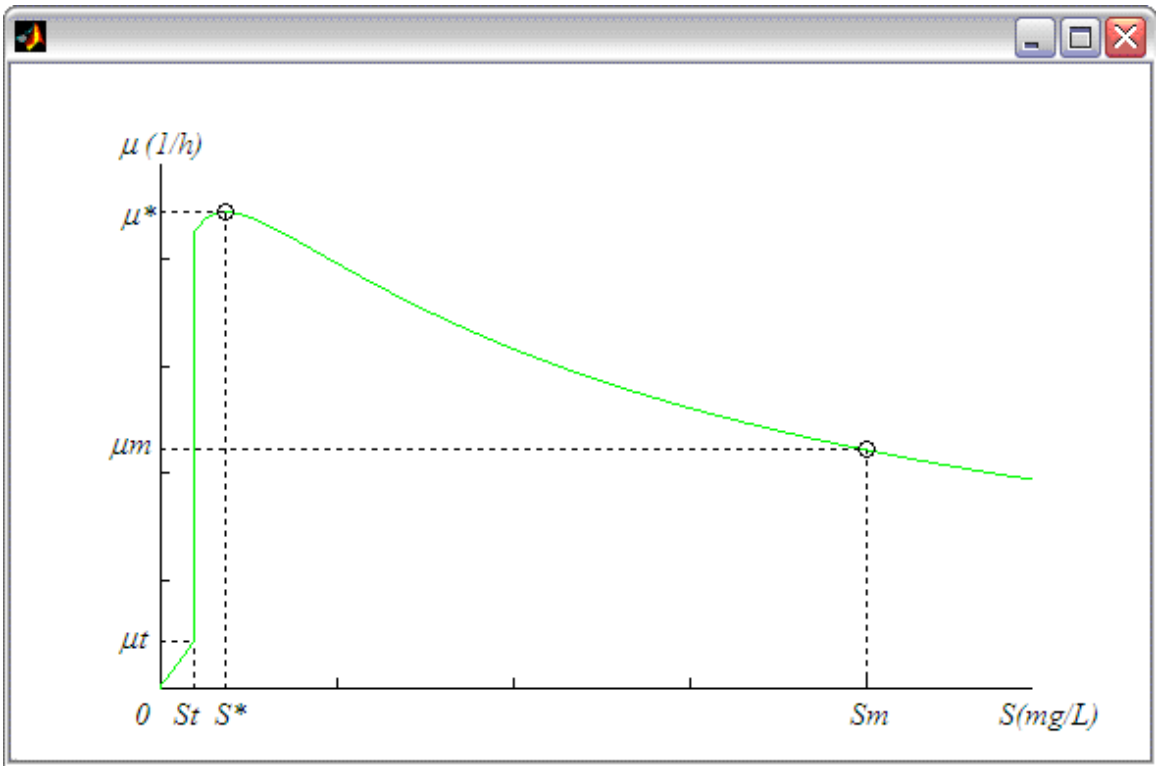

Figure 1. Graph of Eq. 5 representing μ_s for procedure C proposal.
By definition $\mu_m=\mu^*/2$ and $\mu_t=\mu^*/10$
See annex 5 for equivalences with K_I, K_S and μ_o
For procedures A, B and D make $S_t=0$ to obtain the Haldane standard graph.

IDENTIFICATION PROCEDURES

Each EM1 candidate is made by combining two procedures, one for the Yield coefficients (tagged with numbers) and other mainly for the kinetic ones (tagged with letters). This work is concerned with procedures BC3, C3 and D3. However, for completeness, all procedures options are described in Table 1 (for Yield parameters) and Table 2 (for Kinetic parameters).

Table 1. Yield coefficients Estimation/Identifying procedures.

Version	Procedure (Yield coefficients)
1	K_1=3,7 mg4CP/mgVSS is estimated from data coming from a series of batches where total substrate consumption and total biomass generation was measured. See Annex 3.1. K_2 is calculated using the identified relation k_2 / k_1 using the separation technique.
2	K_1 and k_2 are calculated from stechiometric relation (Gaudy et al, 1988) and the identified relation k_2 / k_1. See Annex 3.2.
3	K_1=3,7 mg4CP/mgVSS is estimated from data coming from a series of batches where total substrate consumption and total biomass generation was measured. See Annex 3.1. k_2 is identified using the same program as for kinetic parameters (no separation).

Table 2. Kinetic coefficients identifying procedures.

Version	Procedure (Kinetic coefficients)
A	FTC experiments ID1 and ID2 are used. See Annex 1 for experiment classification. Influent's Oxygen assumed negligible Experiment VAL1 is used for validation
B	FTC experiments ID1 and ID2 are used. See Annex 1 for experiment classification. Influent's Oxygen assumed unknown, but constant for each reaction. Experiment VAL1 is used for validation
BC	Is a combination of B and C i.e. it includes ID1, ID2, ID3, ID4, VAL1 and VAL2
C	FTC experiments ID3 and ID4 are used. See annex 1 for experiment classification. A mathematical model for representing the D.O. sensor is added. A piece-wise discontinuity to μ(S) is added. Experiment VAL2 is used for validation
D	Similar to procedure B, but applied to different experiments. FTC experiments ID3 and ID4 are used. See annex 1 for experiment classification. Experiment VAL2 is used for validation

Initial conditions and estimable parameters for procedure C and D are treated in a similar way as for procedures A and B. See Annex 7. The added filter, that emulates the sensor effect on the measured Oxygen in procedure C, is initialized to S_{Oo} value. D.O. sensor's model identification is described in Annex 8.

A kinetic parameter *"St"* is added to modify the Haldane curve by creating a piecewise discontinuity at low substrate concentrations. This parameter should be identified also.

Fitting criteria and software description is similar to the one used for procedures A and B. See Annex 9 for explanation.

RESULTS AND VALIDATION

Table 3 shows fitting and validation results for EM1-C3 and EM-D3 candidates. For completeness and for comparison all former results are also listed. It can be seen that C3 fits the best and validates the best (i.e. displays the lowest Mean Quadratic Error (MQE)). Table 4 shows the improvement in fitting for EM1-C3 compared to EM1-D3. It is about 18% for the global evaluation, i.e. fitting infinite time horizon (ITH) simulations, using the same single EM1 model under test, for all ID and VAL experiments involved. MQE improvement may go as high as 35% for individual experiments. Table 5 shows all results for all identified parameter values, for all EM1 candidates, and their respective confidence intervals.

Table 3. Validation fitting results for EM1 model candidates using *Fit_SO* criteria

EM1 candidate	Experiment tag	MQE kid (own_parameters)	MQE test (using_EM1)	Mean EM1 test MQE	
				by group	Global
A1	ID1	758	961	804	707
	ID2	812	647		
	VAL1		514	514	
A2	ID1	742	929	788	701
	ID2	794	647		
	VAL1		527	527	
A3	ID1	444	446	392	430
	ID2	328	337		
	VAL1		506	506	
B1	ID1	369	515	390	343
	ID2	373	264		
	VAL1		251	251	
B2	ID1	355	516	383	342
	ID2	353	250		
	VAL1		259	259	
B3	ID1	220	231	186	244
	ID2	127	141		
	VAL1		360	360	
(Unifying) BC3	ID1	220	1339	1512	1525
	ID2	127	1158		
	ID3	12	1824		
	ID4	27	1727		
	VAL1		1866	1550	
	VAL2		1233		
C3	ID3	12	42	51	81
	ID4	27	60		
	VAL2		141	141	
D3	ID3	17	49	58	99
	ID4	41	66		
	VAL2		182	182	

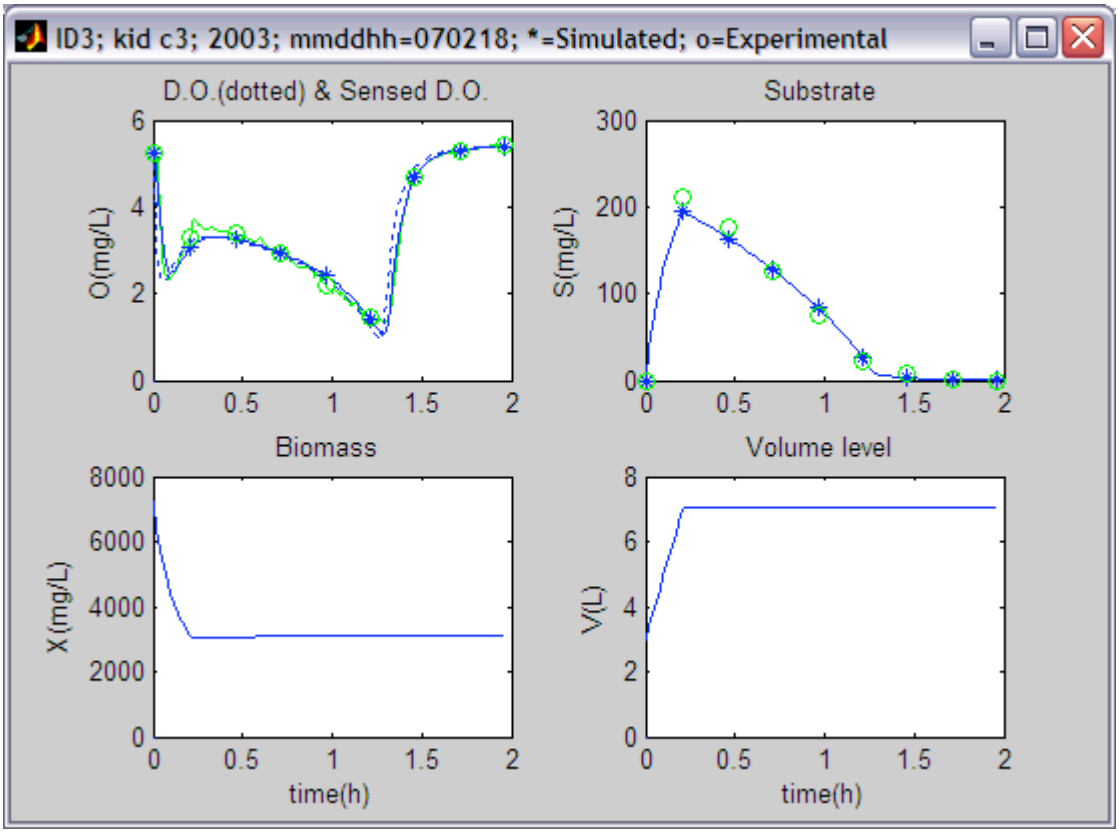

Figure 2. ITH simulation result compared to experimental data for C3 identification of ID3experiment.

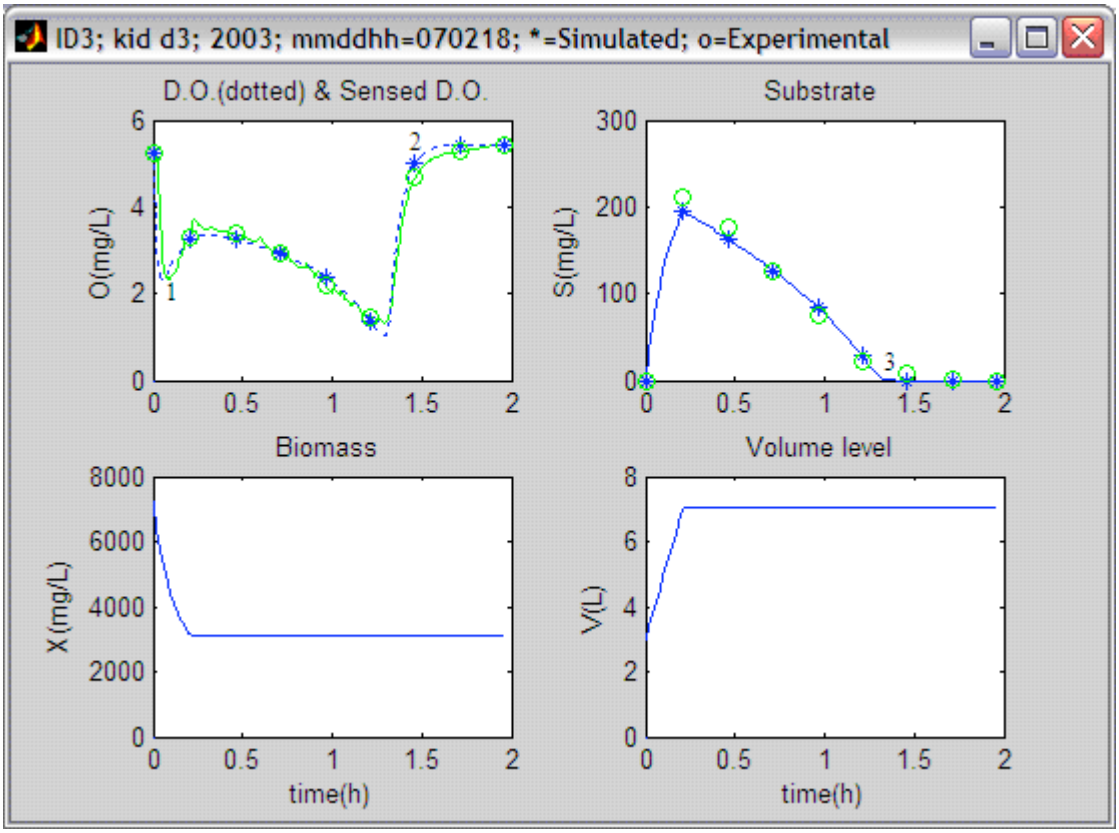

Figure 3. ITH simulation result compared to experimental data for D3 identification of ID3 experiment.

Table 4. Fitting Improvement for EM1-C3 compared to EM1-D3

Fit to	"C3" over "D3" MQE Improvement
kid ID3	31%
kid ID4	35%
test VAL2	22%
Global test	18%

Figure 2 shows the result for ID3 identification using procedure C3, and Figure 3 shows the same experiment with procedure D3. Validation tests for resulting candidates EM1-C3 and EM1-D3 are shown in Figures 4 and 5.

For Figure 2 the fitting graph is the continuous blue line (D.O. sensor simulation), while for Figure 3 the fitting graph is the dotted blue one (without D.O. sensor simulation). The green line is the experimental on-line D.O., and the marked points indicate the manual off-line samplings. There are 3 key-points to compare between Figures 2 and 3. Those will explain the improving mechanism of the EM1-C3 added features and their possible practical implications with respect to EM1-D3:

1. The initial drop of the D.O. right after t_o and into first D.O. valley. See number "1" inside subfigure D.O. of Figure 3. This happens because the system is first quickly gaining activity and then crossing the optimal operational point as S increases, so there is a big D.O. initial demand. EM1-D3 (Fig. 3) represents this without considering the sensor. Any system (software sensors, controllers, supervisory or fault detection systems) using such model will have a response delay error if it uses the real sensed D.O. instead of the "real D.O.". On the contrary, EM1-C3 does represent this filtering (Fig. 2). Hence, if EM1-C3 is used, better practical results are to be expected.

2. Entrance to the last D.O. plateau when reaction is about to finish. See number "2" inside subfigure D.O. of Figure 3. Real D.O. suggest that there is some activity going on at this point as saturation is usually not achieved as quick as EM1-D3 would predict. Instead, EM1-C3 (continuous blue line) in Fig. 2 represents this phenomena by means of the threshold S_t in $\mu(S)$

3. Substrate depletion point. See number "3" inside subfigure Substrate of Figure 3. This is directly related to point 2. Real kinetics display slowly disappearing remaining substrate after the main reaction. By considering it less error in predicting the reaction's finishing time is expected, if finalization criterion happens to be below S_t.

Names of documents, graphs, datasheets etc. are provided in Annex 10.

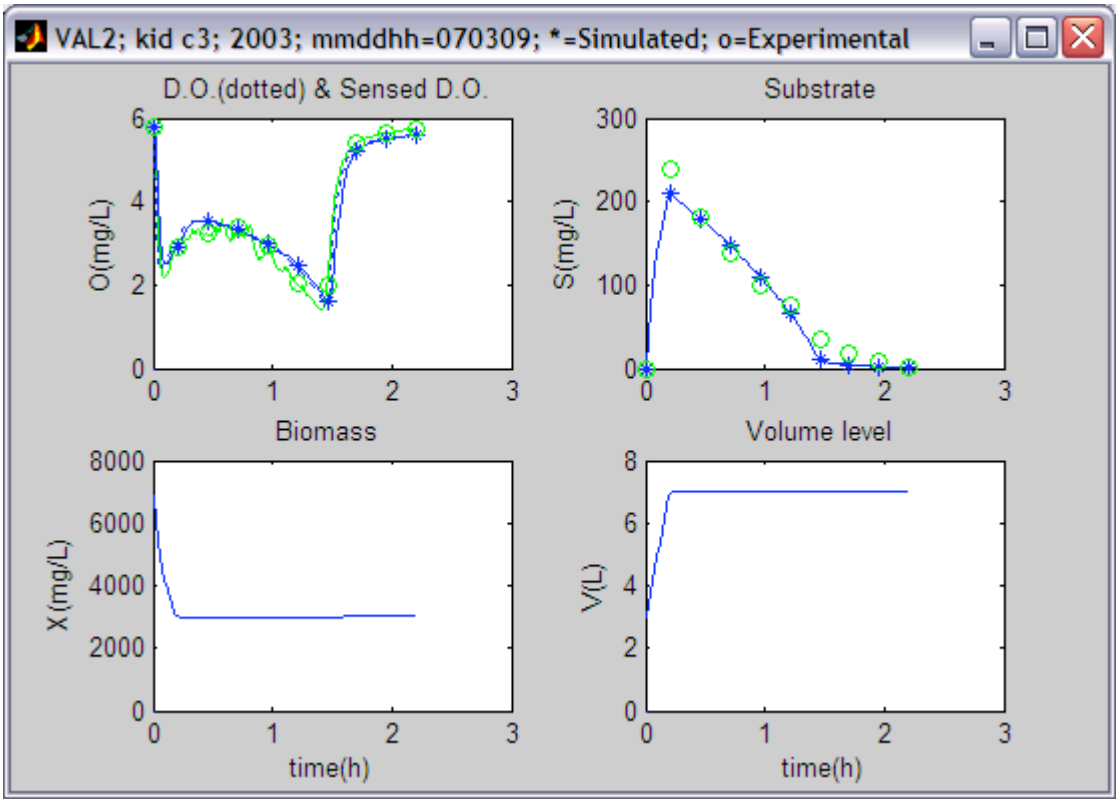

Figure 4. EM1-C3 infinite time horizon (ITH) simulation result compared to VAL2 experimental data for validation.

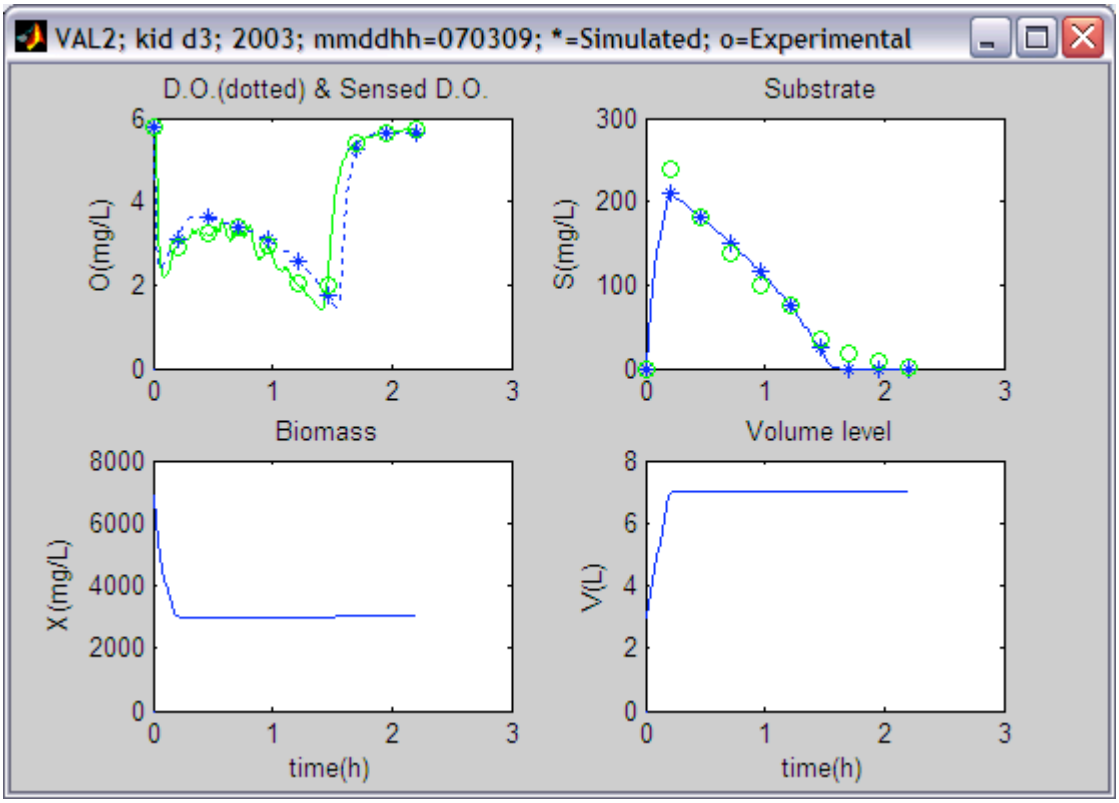

Figure 5. EM1-D3 ITH simulation result compared to VAL2 experimental data for validation.